Valley Zeeman energy in monolayer MoS_2 quantum rings: Aharonov-Bohm effect

D. Oliveira,[1] Jiyong Fu,[1,2] L. Villegas-Lelovsky,[1] A. C. Dias,[1] and Fanyao Qu[1,*]
[1]*Instituto de Física, Universidade de Brasília, Brasília-DF 70919-970, Brazil*
[2]*Department of Physics, Qufu Normal University, Qufu, Shandong, 273165, China*
(Received 1 February 2016; revised manuscript received 3 April 2016; published 12 May 2016)

We investigate the valley Zeeman energy (VZE) in monolayer MoS_2 quantum rings, subjected to a magnetic flux Φ only passing through a hole region enclosed by the inner circle of the ring. To gain insight on our numerical outcomes for finite two-dimensional rings, an analytic solution in the one-dimensional limit (zero ring width) is also presented. Although no magnetic field is applied inside the ring region, we observe finite VZEs. Interestingly, in contrast to the usual linear scenario, the VZE of the rings exhibits an oscillatory dependence on Φ with possible vanishing valley Zeeman effect even in a nonzero magnetic flux due to Aharonov-Bohm type effect. On the other hand, within one period of oscillations the VZE increases linearly with Φ. Furthermore, for a given magnetic flux, the valley Zeeman effect is more pronounced in a ring with a stronger quantum confinement. Thus the VZE can be tuned by either magnetic flux or ring confinement or both of them. This opens a new route for controlling the valley Zeeman effect using a *nonmagnetic* means.

DOI: 10.1103/PhysRevB.93.205422

I. INTRODUCTION

Recently monolayer transition metal dichalcogenides (TMDs) have attracted considerable interest due to their rich electronic and optical properties [1–3]. The lack of lattice inversion symmetry together with strong spin-orbit coupling results in coupled spin and valley pseudospin physics [4–7], making it possible to simultaneously control the real spin and valley pseudospin in these materials [8,9].

For free monolayer TMDs, a variety of achievements such as valley-selective luminescence [10–13], valley coherence [2,14], valley Hall effect [15], and valley Zeeman splitting [16–19], have been demonstrated both theoretically [20] and experimentally [10,16]. In addition, monolayer TMD quantum dots [21,22] have also drawn a lot of attention in the last two years because (i) they open a platform to study spin and valley pseudospin physics in strong confinement systems [23] and (ii) potential applications in single electron and single phonon sources with versatile controllability by varying external confinements. In both two-dimensional (2D) bulk TMDs and their corresponding quantum dots, the magnetic field B induced valley Zeeman energy (VZE), as a key element in the valley manipulation, has been found simply increasing linearly with B [16,24].

In comparison with quantum dots, quantum rings possess several unique properties. For instance, they allow a transition from two dimensions (finite radius-to-width ratio) to a one-dimensional (1D) limit (zero width) by varying the geometry of rings. The latter has simple analytic solutions, which is an ideal platform to understand fundamental spin and valley physics. Furthermore, quantum rings make it possible to explore the valley Zeeman effect entirely due to the Aharonov-Bohm type effect. These advantages motivate us to focus our attention on monolayer TMD quantum rings in which a magnetic flux Φ only passes through the inner circle enclosed hole region ($r < R_1$) (Fig. 1). Interestingly, although there is no flux threading the ring region ($R_1 < r < R_2$), we observe finite valley Zeeman splittings. In addition, it is found that the VZE exhibits an oscillatory behavior with Φ, in contrast to the usual monotonous linear scenario [16,18,23]. On the other hand, within one period of oscillations, the VZE increases linearly with the magnetic flux. Besides, we observe that the VZE can be tuned by varying the geometry of rings which determines ring confinements.

II. THEORETICAL FRAMEWORK

In the vicinity of the K ($\tau = 1$) and K' ($\tau = -1$) valleys, by constructing the wave functions through the basis of conduction and valence bands, an effective two-band Hamiltonian for 2D bulk TMDs can be obtained from density functional theory calculations [8,9]. Accordingly, for our quantum rings (Fig. 1) the low-energy effective Hamiltonian reads

$$\mathcal{H} = \mathcal{H}_0 + \frac{\Delta}{2}\hat{\sigma}_z + \frac{\lambda_{so}}{2}\tau\hat{s}_z(1-\hat{\sigma}_z) + V(\mathbf{r})\hat{\sigma}_z, \qquad (1)$$

where $\mathcal{H}_0 = \hbar v_F(\tau\hat{\sigma}_x k_x + \hat{\sigma}_y k_y)$, v_F denotes the Fermi velocity given by $v_F = at/\hbar$ with t as the effective hopping integral and a as the lattice constant, and $\hat{\sigma}_{x,y,z}$ are the Pauli matrices, acting on the atomic orbitals. Since spin is a good quantum number, $s_z = \pm 1$ stand for states of spin up and spin down.

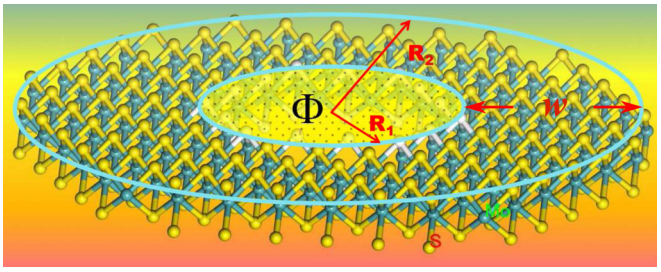

FIG. 1. Schematic of a monolayer MoS_2 circular quantum ring with inner radius R_1, outer radius R_2, and width $w = R_2 - R_1$. A magnetic flux Φ only threads the hole region ($r < R_1$) enclosed by the inner circle of the ring, as indicated by the dotted region.

*fanyao@unb.br

$\hbar\mathbf{k} = -i\hbar\nabla + e\mathbf{A}$ is the kinetic momentum, with $e > 0$ as the electron charge and $\mathbf{A}$ as the vector potential describing a magnetic flux. Δ represents the energy gap and λ_{so} denotes the spin-orbit coupling constant. $V(\mathbf{r})$ is the confinement potential of the ring, defined by $V(\mathbf{r}) = 0$ for $R_1 \leqslant |\mathbf{r}| \leqslant R_2$, otherwise $V(\mathbf{r}) = \infty$, as shown in Fig. 1.

By defining a valley dependent angular momentum as $J^\tau_{\text{eff}} = L_z + \hbar\tau\sigma_z/2$, we find $[\mathcal{H}, J^\tau_{\text{eff}}] = 0$, with L_z as the orbital angular momentum along the z direction. This results in common eigenstates $|\psi^\tau_m\rangle$ of J^τ_{eff} and $\mathcal{H}$, i.e., $J^\tau_{\text{eff}}|\psi^\tau_m\rangle = m\hbar|\psi^\tau_m\rangle$ and $\mathcal{H}|\psi^\tau_m\rangle = E|\psi^\tau_m\rangle$. We consider that an applied magnetic flux Φ only threads a disk region enclosed by the inner circle of rings, as shown in Fig. 1. In the polar coordinate system (r, ϕ) and in the Landau gauge defined by $\vec{A} = (\Phi/2\pi r)\vec{e}_\phi$, the Hamiltonian $\mathcal{H}$ reads

$$\mathcal{H} = \begin{pmatrix} \frac{\Delta}{2} & \Pi^\dagger_+ \\ \Pi_+ & -\frac{\Delta}{2} + \tau s_z \lambda_{\text{so}} \end{pmatrix}, \tag{2}$$

with

$$\Pi_+ = -iate^{i\tau\phi}\left(\tau\frac{\partial}{\partial r} + \frac{i}{r}\frac{\partial}{\partial\phi} - \frac{\Phi}{\Phi_0}\frac{1}{r}\right). \tag{3}$$

Because of the rotational symmetry of the ring confinements, the wave function of $\mathcal{H}$ admits the following *Ansatz*:

$$\psi^\tau_m(r,\phi) = e^{i(m-\tau/2)\phi}\begin{pmatrix} a_\tau(r) \\ e^{i\tau\phi}b_\tau(r) \end{pmatrix}, \tag{4}$$

where $a_\tau(r)$ and $b_\tau(r)$ are the radial components of pseudospinnor and $m = \pm 1/2, \pm 3/2, \ldots$ refers to the total angular momentum.

After some algebra calculations, a general form of eigenstates is obtained as

$$\psi_\tau(\rho,\phi) = \alpha_\tau e^{i(m-\tau/2)\phi}\begin{pmatrix} H^{(1)}_{\bar{m}-\tau/2}(\sqrt{\gamma}\rho) \\ c_E e^{i\tau\phi}H^{(1)}_{\bar{m}+\tau/2}(\sqrt{\gamma}\rho) \end{pmatrix} + \beta_\tau e^{i(m-\tau/2)\phi}\begin{pmatrix} H^{(2)}_{\bar{m}-\tau/2}(\sqrt{\gamma}\rho) \\ c_E e^{i\tau\phi}H^{(2)}_{\bar{m}+\tau/2}(\sqrt{\gamma}\rho) \end{pmatrix}, \tag{5}$$

where $H^{(1)}_\nu$ ($H^{(2)}_\nu$) are Hankel functions of the first (second) kind, $\gamma = (s_E - \delta)(\delta - \lambda s_z\tau + s_E)$, $c_E = i(s_E - \delta)/\sqrt{\gamma}$, $\bar{m} = m + \Phi/\Phi_0$ refers to an *effective* quantum number, with $\Phi_0 = 2\pi\hbar/e$ as the elementary flux, α_τ and β_τ are normalization constants. To facilitate our calculation, unless stated otherwise, the following dimensionless quantities: $s_E = \text{sgn(E)}$, $\delta = \Delta/2|E|$, $\lambda = \lambda_{\text{so}}/|E|$, and $\rho = |E|r/at$, are adopted.

With the general expression of $\psi_\tau(\rho,\phi)$ at hand, the eigensolution of $\mathcal{H}$ can be obtained by applying the infinite mass boundary condition, i.e., $b(R_2) = i\tau a(R_2)$ and $b(R_1) = -i\tau a(R_1)$, at the outer and inner boundaries, respectively. The secular equation corresponds to $z_1 = z_2$, where z_j is given by

$$z_j = \frac{H^{(j)}_{\bar{m}-\tau/2}(\sqrt{\gamma}\rho_2) + ic_E\tau H^{(j)}_{\bar{m}+\tau/2}(\sqrt{\gamma}\rho_2)}{H^{(j)}_{\bar{m}-\tau/2}(\sqrt{\gamma}\rho_1) - ic_E\tau H^{(j)}_{\bar{m}+\tau/2}(\sqrt{\gamma}\rho_1)}. \tag{6}$$

It is worth commenting that in a special case such as graphene ring in which $\Delta \to 0$, $\lambda_{\text{so}} \to 0$ and $\tau = 1$, the constants γ and c_E determining the eigenstates change accordingly as $\gamma \to 1$ and $c_E \to is_E$, and our results reduce to those of the graphene ring shown in Ref. [25].

To gain insight on our numerical outcomes, let us derive an analytic expression of the eigensolution for a thin ring with negligible width which arrives at the 1D limit. It can be implemented by freezing out carrier radial motions in the Schrödinger equation for rings of finite width,

$$E_\pm = \frac{\lambda_{\text{so}}s_z\tau}{2} \pm t\sqrt{\left(\bar{m}^2 - \frac{1}{4}\right)\left(\frac{a}{R_t}\right)^2 + \left(\frac{\Delta - \lambda_{\text{so}}s_z\tau}{2t}\right)^2}, \tag{7}$$

with the radius $R_t \sim R_1 \sim R_2$. Note that the energies of the lowest conduction band and the highest valence band corresponding to $\bar{m} = \pm 1/2$ are given by $E_+ = \Delta/2$ and $E_- = -\Delta/2 + \lambda_{\text{so}}s_z\tau$, which do not depend on the geometry of rings, in contrast to all other states for which $\bar{m} \neq \pm 1/2$, energies strongly dependent on the geometry parameters of the ring, see Eq. (7).

III. SYSTEM

We consider MoS_2 quantum rings, with the inner and outer radius of R_1 and R_2, respectively, and the width $w = R_2 - R_1$, as shown in Fig. 1. We assume that an applied magnetic flux Φ only passes through a disk region enclosed by the inner circle (i.e., $r < R_1$), allowing us to explore the valley Zeeman energy entirely due to the Aharonov-Bohm type effect. The ring width w and average radius $R_a = (R_1 + R_2)/2$ are two major quantities used to measure a ring confinement. In our numerical simulation, we use the following typical parameters for a monolayer MoS_2, $t = 1100$ meV, $a = 0.3193$ nm, $\Delta = 1660$ meV, and $\lambda_{so} = 75$ meV.

IV. ZERO FIELD ENERGY SPECTRUM

In Fig. 2(a) we show the energy spectrum of the lowest three conduction bands and the highest three valence bands as functions of the angular momentum m, for the spin up state in the K valley ($\tau = 1, s_z = 1$) and the spin-down state in the K' valley ($\tau = -1, s_z = -1$). Since the confinement potential couples with the orbital pseudospin, Eq. (1), the *effective* time reversal symmetry (TRS) is broken within a single valley even in the absence of a magnetic field/flux, similar to graphene quantum dots/rings [25]. As a consequence, in a single valley the dependence of energy on m is asymmetric referring to $\pm m$, i.e., $E^\tau(m) \neq E^\tau(-m)$ for both the conduction and valence bands. However, since the real TRS preserves at zero magnetic field/flux, the equality $E^\tau(m) = E^{-\tau}(-m)$ involving two distinct valleys still holds, as expected. In addition, the energy spectrum in Fig. 2(a) also shows that the particle-hole symmetry is broken, cf. conduction and valence-band spectra, because the inversion asymmetry of the crystal structure, spin-orbit interaction, and confinement potential do not commute with the *effective* inversion symmetry operator defined in a single valley given by $P_e = I_\tau \otimes \sigma_x$, with I_τ as the identity matrix.

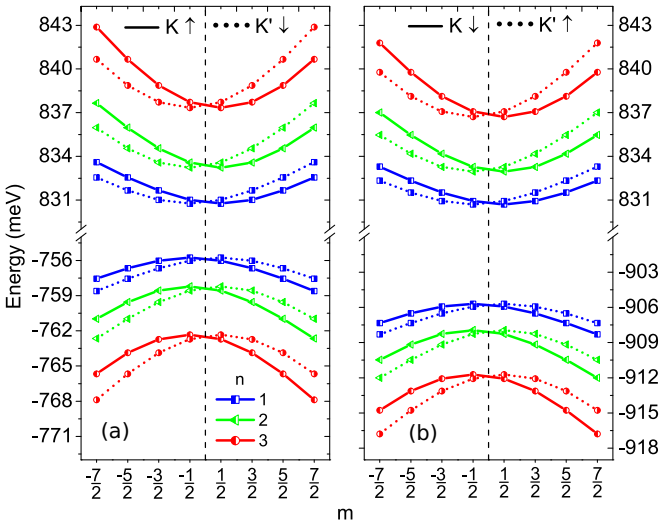

FIG. 2. Energy spectrum as a function of the angular momentum m at $\Phi = 0$ for (a) (K, spin up) and (K', spin down) states and (b) (K, spin down) and (K', spin up) states, for the first three quantum states denoted as $n = 1,2,3$. The ring has an average radius $R_a = 20$ nm and a width $w = 30$ nm.

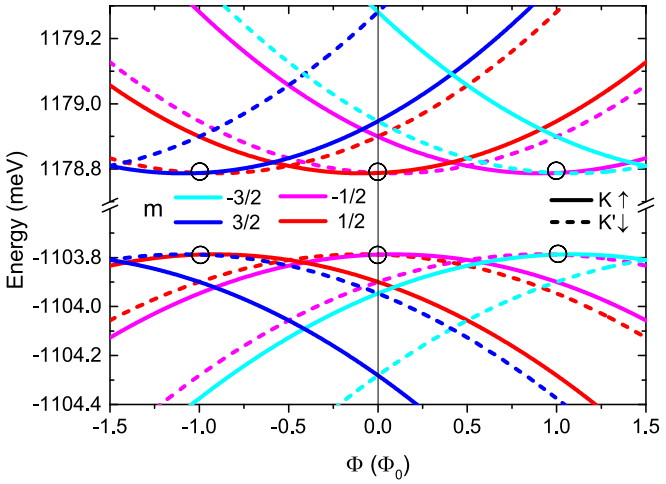

FIG. 3. Energy spectrum in a quantum ring of $R_a = 20$ nm and $w = 1$ nm as a function of the magnetic flux Φ (in unit of elementary flux Φ_0) for (K, spin up) and (K', spin down) states. Several values of m's, with $m = \pm 1/2, \pm 3/2$, are considered. The black circles indicate different states that have the same energy for both the lowest conduction band and the highest valence band.

In Fig. 2(b) we show the corresponding analogs to the energy spectrum in Fig. 2(a) but for the K valley with spin down ($\tau = 1$, $s_z = -1$) and the K' valley with spin up ($\tau = -1$, $s_z = 1$). We find similar behaviors of E versus m to that for ($\tau = 1$, $s_z = 1$) and ($\tau = -1$, $s_z = -1$), cf. Figs. 2(a) and 2(b).

Furthermore, by comparing Figs. 2(a) and 2(b), we find that conduction-band energies for the spin up and spin down states in the same valley are close but different for most values of m's, and the distinction ($\sim$meV) is more considerable for a larger value of m. Since in our model there is no direct spin-orbit term for the conduction band right at the K (or K') valley [Eq. (1)], we attribute the spin splitting to the ring confinement, for both spin states. To facilitate understanding this, we get help from an analytic solution in the 1D limit, see Eq. (7), where the ring confinement and magnetic flux induced energy correction is determined by the first term [$\propto (a/R_t)^2$] inside the square root which contains $\bar{m}$. At zero flux, $\bar{m} = m$ and the energy correction increases with m, thus leading to a stronger spin splitting in a single valley for a larger angular momentum. Physically we emphasize that the energy correction arises from the fact that the Hamiltonian $H_0 + V(\mathbf{r})\hat{\sigma}_z$ does not commute with the spin-orbit term, see Eq. (1). Accordingly, although there is no direct spin-orbit contribution in the conduction band, the corresponding states are still spin mixed. Note that the energy correction vanishes at $\bar{m} = \pm 1/2$, corresponding to the case that the *effective* pure orbital angular momentum is zero [Eq. (7)]. As for the valence band, the distinction of the energy spectrum between the spin up and spin down states in a given valley, is dominated by the spin-orbit term λ_{so}.

V. EFFECT OF MAGNETIC FLUX ON ENERGY SPECTRUM

Figure 3 shows the energy spectrum of the lowest conduction band and the highest valence band for the (K, spin up) and (K', spin down) states, as a function of magnetic flux. At $\Phi = 0$, the states in distinct valleys with opposite spin and angular momentum have the same energy for both the conduction and valence bands, i.e., $E^{K}_{c/v,\uparrow}(m = 1/2) = E^{K'}_{c/v,\downarrow}(m = -1/2)$, due to the TRS. Here the subscripts c and v stand for conduction and valence bands, respectively. When Φ deviates from zero, the magnetic flux breaks the TRS, and hence the energy degeneracy between $E^{K}_{c/v,\uparrow}(m = 1/2)$ and $E^{K'}_{c/v,\downarrow}(m = -1/2)$ in general is lifted. However, interestingly the degeneracy can still possibly remain for a nonzero flux Φ being integer multiples of the elementary flux Φ_0, i.e., $\Phi/\Phi_0 = k$ with k an integer, see black circles in Fig. 3. This arises from the periodic dependence of the energy spectrum on the applied magnetic flux. Since the energy spectrum of our rings depends on an *effective* angular momentum, $\bar{m} = m + \Phi/\Phi_0$, renormalized by the magnetic flux [Eq. (6)], the periodic behavior of the energy versus Φ with a period of Φ_0 follows. Physically, the periodic dependence of energy spectra on Φ is originated from the Aharonov-Bohm type effect, which involves a phase variation of the states when Φ changes.

VI. CONTROL OVER VZE: AN INTERPLAY OF MAGNETIC FLUX AND RING CONFINEMENT

Now we turn to the valley Zeeman energy referring to the lowest conduction band (ΔE_c) and the highest valence band (ΔE_v), which is a key ingredient in controlling the valley degree of freedom. The valley Zeeman energy $\Delta E_{c/v}$ is defined as the energy splitting of the corresponding band with opposite spin in distinct valleys, i.e., $\Delta E_{c/v} = E^{K}_{c/v,\uparrow} - E^{K'}_{c/v,\downarrow}$. From our model, the results show that $\Delta E_c \sim \Delta E_v$. Therefore, below we only focus on $\Delta E \equiv \Delta E_v$, as illustrated in Fig. 4(a).

In Fig. 4(b) we show the VZE as a function of magnetic flux, for rings with average radius $R_a = 8$ and 15 nm,

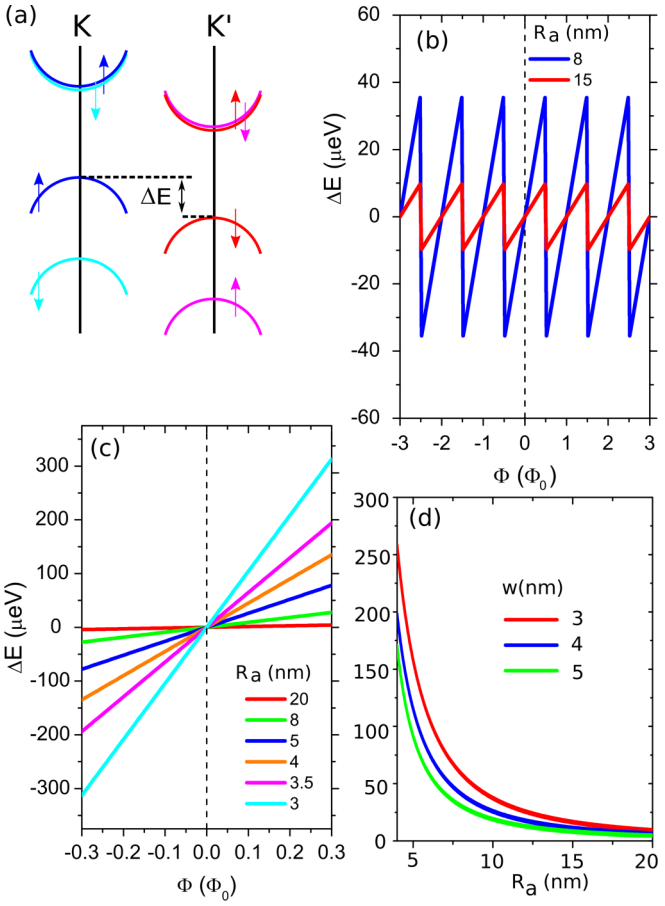

FIG. 4. (a) Schematic diagram of the band structure and valley Zeeman energy, around the K and K' points. Up and down arrows represent the spin states. (b) Valley Zeeman energy as a function of magnetic flux Φ in a quantum ring of $w = 4$ nm and $R_a = 8$ nm (blue curve) and 15 nm (red curve). (c) Valley Zeeman energy versus Φ within only one period of oscillations in a quantum ring at $w = 4$ nm for several values of R_a's. (d) Valley Zeeman energy versus R_a at $\Phi/\Phi_0 = 0.45$ for $w = 3,4,5$ nm, respectively.

respectively. Although the flux only passes through a disk region enclosed by the inner circle of the rings, interestingly we observe a remarkable valley Zeeman effect, which is attributed to the Aharonov-Bohm type effect. Moreover, the VZE exhibits an oscillatory behavior with Φ, with a period of Φ_0. This oscillation straightforwardly arises from the periodic dependence of the energy spectrum on magnetic flux, as we have discussed above. Note that the valley Zeeman effect vanishes at $\Phi = 0$. Because of the oscillation of the VZE with Φ, the VZE can possibly be zero even for nonzero magnetic flux Φ being integer multiples of Φ_0.

Furthermore, by comparing the VZE for rings of $R_a = 8$ and 15 nm in Fig. 4(b), we find that the valley Zeeman effect is enhanced, in a ring with smaller average radius which has stronger confinements. On the other hand, the oscillation period of VZE versus Φ is independent of the geometry of rings, which remains Φ_0 for rings of any sizes. The underlying cause of the oscillation period equal to the Φ_0 is as follows. The phase shift induced by the vector potential on an electron propagating once around a closed loop is given by $e/\hbar \oint \mathbf{A} \cdot \mathbf{dl} = 2\pi\Phi/\Phi_0$. Hence the phase difference equals 2π times the enclosed flux in units of the flux quantum Φ_0. As a phase difference is only distinguishable Mod(2π), any effect resulting from this enclosed flux will show a periodic behavior, with a period of one flux quantum. This conclusion can also be drawn from our eigensolutions of the rings, which are characterized by the effective quantum number $\bar{m} = m + \Phi/\Phi_0$, in both the general 2D ring with finite width [Eq. (6)] and the 1D limit [Eq. (7)]. Therefore, states with the same $\bar{m}$ but with different combinations of m and Φ/Φ_0 have the same energy, e.g., $E(m,\Phi/\Phi_0) = E(m-1,\Phi/\Phi_0+1)$, implying a Φ_0 periodicity of the dependence of energy spectra on magnetic flux.

In Fig. 4(c) we show the VZE as a function of Φ for several values of R_a's, within one period of oscillation, i.e., $|\Phi| < \Phi_0$. In this range we find that the VZE increases linearly with Φ. Moreover, the VZE in rings of smaller R_a is found more sensitive to a variation of Φ than that in larger rings, cf. slopes of VZE versus Φ for rings of different R_a's.

To get an insight into the VZE in the ring, we have also performed the calculations in both quantum dots and in the 2D bulk subjected to perpendicular magnetic fields. More specifically, for the 2D bulk, the energy spectrum is given by $E_n = \lambda_{so}\tau s_z/2 + \sigma_z\sqrt{(\Delta - \lambda_{so}\tau s_z)^2/4 + t^2a^2\omega_c^2 n}$ at the low energy region, n is the Landau level index, and $\omega_c = \sqrt{2}/l_B$. Thus it is straightforward to obtain the field dependence of VZE, $\Delta E/\Delta B \approx [2/(\Delta - \lambda_{so})](t^2a^2/25.6^2) \sim 238\ \mu$eV/T [26], close to the experimental value 200 μeV/T [24]. On the other hand, for a 40-nm quantum dot, we find the slope of VZE versus B is similar to the bulk case. In addition, based on the B field dependence of VZE, one can further extract the valley g_v factor, i.e., $\sim$4.11 for the dot and bulk cases as expected. This gives strong support for our model calculation. Therefore, we can safely conclude that the magnetic flux in the ring does induce the VZE via Aharonov-Bohm effect, but it is smaller than that in the quantum dots subjected to a magnetic field. Although the Aharonov-Bohm effect induced VZE has a relatively weak dependence on magnetic flux, here we mainly focus on emergent unique properties in quantum rings, e.g., ring-geometry dependent oscillating behavior of VZE with magnetic flux, which does not exist either in the pristine monolayer or in quantum dots.

To gain insight of the dependence of VZE on ring confinement, in Fig. 4(d) we show the VZE as a function of average radius R_a, at a constant flux $\Phi = 0.45\Phi_0$ for several values of ring width w's. For a given w we find that the VZE first decreases with increasing R_a up to 15 nm, as discussed previously. Nevertheless, with a further increase of R_a, the VZE only slightly changes. Similar to the R_a dependence of VZE, the smaller the ring width is, the higher the VZE effect becomes due to an enhanced confinement. In the regime of $w \ll R_a$, which is around 15 nm for rings we focus on here, our system approaches the one-dimensional limit. In this regime the energy for the highest valence band (or the lowest conduction band) only depends on the intrinsic spin and valley degrees of freedom, see Eq. (7), and hence the valley Zeeman energy remains almost a constant as the geometry of rings varies. We should emphasize that the dependence of VZE on ring confinements opens the possibility of controlling the

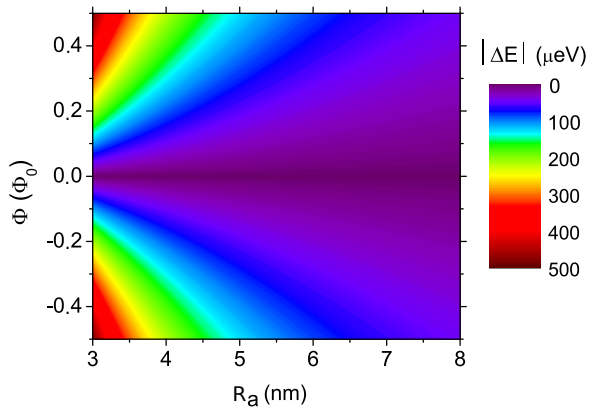

FIG. 5. Cartoon plot of valley Zeeman energy as a function of average radius R_a and magnetic flux Φ in a MoS_2 ring of $w = 4$ nm.

valley degree of freedom using a *nonmagnetic* means for a given magnetic flux.

In order to demonstrate a whole control over the valley Zeeman effect, we show a cartoon plot of VZE as a function of the magnetic flux and average radius for rings with $w = 4$ nm in Fig. 5. Notice that no VZE is available in the case of $\Phi = 0$. For $\Phi \neq 0$, however, a symmetric figure showing the magnitude of valley Zeeman splitting with respect to opposite values of Φ is found. Also note that either Φ or R_a or both of them can be used to tune the VZE.

It is worth addressing that the Zeeman and cyclotron energies are negligible as compared to the band gap, which allows a simple effective-mass model to describe both conduction and valance bands [27,28]. In this effective model, the valley pseudospin in 2D TMDs plays a similar role to the spin degree of freedom in conventional semiconductor quantum rings. Therefore, one can in principle apply the available knowledge (well-established methods and known results) about the conventional rings to investigate TMDs rings [27,28].

Finally, we recall that the two-band model in which the effect of remote band is neglected, yields equal electron and hole mass and equal conduction and valence band g factor around the K and K' points [27,28]. Strictly speaking, the effective mass and g factor depend on the band, valley, and even spin states [22,27]. The approximation of band independent effective mass in our model results in vanishing contribution of valley magnetic moment to the valley Zeeman splitting [24,27]. We emphasize that these neglected effects in our two-band model might give further enhancement of the valley Zeeman effect. However, all of our conclusions remain unchanged.

VII. CONCLUDING REMARKS

We have investigated the valley Zeeman energy (VZE) entirely due to the Aharonov-Bohm type effect in monolayer MoS_2 quantum rings, subject to a magnetic flux only threading the hole region enclosed by the inner circle of rings. The effect of magnetic flux on the energy spectrum has also been discussed. Despite having no flux passing through the ring region, we have observed a remarkable valley Zeeman effect. This unusual VZE exhibits an oscillatory dependence on applied magnetic flux, in contrast to the usual linear scenario. Although the oscillation period is independent of ring confinements, the strength of valley Zeeman splitting can be considerably tuned by the geometry of rings, i.e., ring radius and width. On the other hand, within one period of the oscillation, the VZE shows a linear dependence on applied flux. Since the valley Zeenman energy depends on the combined effect of the magnetic flux and ring confinements, our results are expected to open a route in engineering the spin and valley degrees of freedom in monolayer MoS_2 nanostructures, via a nonmagnetic means. We should emphasize that here we do not consider the situation that a magnetic flux passes through the ring region, which is similar to the case of quantum dots [23]. As a final remark on the practical implementation of magnetic flux which is only restricted to the limited hole region, we suggest using predesigned superconductor rings, where the magnetic field is screened out in the ring region and allowed only in the hole region.

ACKNOWLEDGMENT

This work was supported by CNPq, CAPES, FAPDF, and the Natural Science Foundation of China (Grant No. 11004120).

[1] K. F. Mak, K. He, J. Shan, and T. F. Heinz, Nat. Nanotechnol. **7**, 494 (2012).
[2] A. M. Jones *et al.*, Nat. Nanotechnol. **8**, 634 (2013).
[3] J. Zaumseil, Science **344**, 702 (2014).
[4] X. D. Xu, W. Yao, D. Xiao, and T. F. Heinz, Nat. Phys. **10**, 343 (2014).
[5] G. B. Liu, D. Xiao, Y. G. Yao, X. D. Xu, and W. Yao, Chem. Soc. Rev. **44**, 2643 (2015).
[6] G. B. Liu, W. Y. Shan, Y. G. Yao, W. Yao, and D. Xiao, Phys. Rev. B **88**, 085433 (2013).
[7] A. Splendiani, L. Sun, Y. B. Zhang, T. S. Li, J. Kim, C. Y. Chim, G. Galli, and F. Wang, Nano Lett. **10**, 1271 (2010).
[8] D. Xiao, G. B. Liu, W. X. Feng, X. D. Xu, and W. Yao, Phys. Rev. Lett. **108**, 196802 (2012).
[9] W. Y. Shan, H. Z. Lu, and D. Xiao, Phys. Rev. B **88**, 125301 (2013).
[10] Y. L. Li *et al.*, Phys. Rev. Lett. **113**, 266804 (2014).
[11] T. Cao, G. Wang, W. P. Han, H. Q. Ye, C. R. Zhu, J. R. Shi, Q. Niu, P. H. Tan, E. Wang, B. L. Liu, and J. Feng, Nat. Commun. **3**, 887 (2012).
[12] H. L. Zeng, J. F. Dai, W. Yao, D. Xiao, and X. D. Cui, Nat. Nanotechnol. **7**, 490 (2012).
[13] J. S. Ross, S. F. Wu, H. Y. Yu, N. J. Ghimire, A. M. Jones, G. Aivazian, J. Q. Yan, D. G. Mandrus, D. Xiao, W. Yao, and X. D. Xu, Nat. Commun. **4**, 1474 (2012).
[14] Q. H. Wang, K. K. Zadeh, A. Kis, J. N. Coleman, and M. S. Strano, Nat. Nanotechnol. **7**, 699 (2012).

[15] K. F. Mak, K. L. McGill, J. Park, and P. L. McEuen, Science **344**, 1489 (2014).
[16] D. MacNeill, C. Heikes, K. F. Mak, Z. Anderson, A. Kormányos, V. Zólyomi, J. Park, and D. C. Ralph, Phys. Rev. Lett. **114**, 037401 (2015).
[17] R. L. Chu, X. Li, S. F. Wu, Q. Niu, W. Yao, X. D. Xu, and C. W. Zhang, Phys. Rev. B **90**, 045427 (2014).
[18] G. Aivazian, Z. R. Gong, A. M. Jones, R. L. Chu, J. Yan, D. G. Mandrus, C. W. Zhang, D. Cobden, W. Yao, and X. Xu, Nat. Phys. **11**, 148 (2015).
[19] A. Srivastava, M. Sidler, A. V. Allain, D. S. Lembke, A. Kis, and A. Imamoglu, Nat. Phys. **11**, 141 (2015).
[20] F. C. Wu, F. Y. Qu, and A. H. MacDonald, Phys. Rev. B **91**, 075310 (2015).
[21] G. B. Liu, Q. L. Pang, Y. G. Yao, and W. Yao, New J. Phys. **16**, 105011 (2014).
[22] A. Kormányos, V. Zólyomi, N. D. Drummond, and G. Burkard, Phys. Rev. X **4**, 011034 (2014).
[23] A. C. Dias, J. Y. Fu, L. V. Lelovsky, and F. Y. Qu (unpublished).
[24] A. V. Stier, K. M. McCreary, B. T. Jonker, J. Kono, and S. A. Crooker, Nat. Commun. **7**, 10643 (2016).
[25] P. Recher, B. Trauzettel, A. Rycerz, Ya. M. Blanter, C. W. J. Beenakker, and A. F. Morpurgo, Phys. Rev. B **76**, 235404 (2007).
[26] To obtain the field dependence of VZE in the 2D bulk, we have ignored the term of nonlinear dependence, which is negligibly small.
[27] A. Kormányos, G. Burkard, M. Gmitra, J. Fabian, V. Zólyomi, N. D. Drummond, and V. Fal'ko, 2D Mater. **2**, 022001 (2015).
[28] G. Wang, L. Bouet, M. M. Glazov, T. Amand, E. L. Ivchenko, E. Palleau, X. Marie, and B. Urbaszek, 2D Mater. **2**, 034002 (2015).